

Superradiance and instabilities in black holes surrounded by anisotropic fluids

B. Cuadros-Melgar^{*}

*Escola de Engenharia de Lorena, Universidade de São Paulo,
Estrada Municipal do Campinho S/N,
CEP 12602-810, Lorena, SP, Brazil*

R. D. B. Fontana[†]

*Universidade Federal do Rio Grande do Sul, Campus Tramandaí,
Estrada Tramandaí-Osório, CEP 95590-000, RS, Brazil*

Jeferson de Oliveira[‡]

*Instituto de Física, Universidade Federal de Mato Grosso,
CEP 78060-900, Cuiabá, MT, Brazil*

Abstract

In this paper we analyze the propagation of a charged scalar field in a Reissner-Nordström black hole endowed with one anisotropic fluid that can play the role of a cosmological term for certain set of parameters. The evolution of a scalar wave scattering is examined giving rise to the same superradiant scattering condition as in the de Sitter case. In addition, an analysis of the modes coming from the application of quasinormal boundary conditions is presented. Some special cases displaying analytical solutions for the quasinormal frequencies are discussed. Moreover, the superradiant condition is adapted to the quasinormal problem triggering unstable modes, what is confirmed by our numerical analysis.

^{*} bertha@usp.br

[†] rodrigo.dalbosco@ufrgs.br

[‡] jeferson.oliveira@ufmt.br

I. INTRODUCTION

Black hole solutions are one of the most studied subjects in general relativity along the years. Their physical reality is confirmed by the measurements of gravitational wave signals compatible with a multitude of observations: the binary black hole merger by the LIGO-VIRGO collaboration [1], the first observation of the shadow of the supermassive compact object at the centre of *M87* galaxy done by the EHT collaboration [2], and the evidence that Sagitarius A* is a black hole observed by the GRAVITY collaboration [3].

The gravitational wave signal due to a binary black hole merger is strong enough to permit the observation of its ringdown phase described by the quasinormal modes (QNMs) of the system [4]. The QNMs, damped oscillatory solutions of a particular wave equation, are very well studied in the literature since the seminal work of Regge and Wheeler [5]. In such work the stability of Schwarzschild 'singularity' is analyzed under a gravitational perturbation given rise to gravitational potentials of the wave equation. Furthermore, in the context of AdS/CFT correspondence it is noteworthy to mention the remarkable interpretation of the fundamental QNMs frequencies as the relaxation time scale of a perturbed finite temperature quantum field theory [6–8]. Most recently QNMs were proven to be connected with geometrical properties of the spacetime as well [9–12].

The question of black holes stability against perturbations can be explored through the computation of QNMs [13]. Due to the open nature of the physical region, since the perturbations can be absorbed by the event horizon or scattered to infinity, the QNMs spectrum is given by a set of complex frequencies $\omega = \omega_R - i\omega_I$. In the case of stability the imaginary part of the QNMs spectrum is positive ($\omega_I > 0$) featuring decaying modes. Otherwise, the presence of growing modes indicates that the system is unstable since physical quantities do not remain bounded for all times. Examples of unstable field evolutions include the Kerr black hole with massive scalar field perturbations [14] and the Reissner-Nordström-de Sitter geometry under massive charged scalar field perturbation, which presents growing modes turning the system unbounded [15–17]. The origin of those instabilities is the phenomenon of superradiance [18], which in general is a feature of dissipative systems, where a scattering process could lead to the extraction of black hole energy [19–23], thus increasing the strength of the scattered wave.

As pointed out by Teukolsky and Press [24], if the enhanced wave is continuously scat-

tered back to the black hole event horizon (by a spherical reflective mirror placed at some finite radius r_0 , for example), then, the total energy extracted from the black hole grows exponentially leading to an unstable system known as black hole bomb. A similar situation can be found in the cases of rotating AdS black holes, where the AdS boundary acts as a wall [25] and in the superradiant scattering of massive scalar waves, in which the mass term acts a potential barrier [26].

In the astrophysical context stellar black holes are expected to be surrounded by matter (fluids), in that sense the family of exact solutions discovered by Kiselev [27] describing black holes surrounded by anisotropic fluids can be considered as an approximate model. The question of its stability was studied in [28–32] and the QNMs spectrum due to massless scalar perturbations, the late-time tails structure, and some thermodynamical aspects were presented in [33].

In the present work we perform a further investigation on the dynamics of a probe scalar field in the spacetime of black holes surrounded by anisotropic fluids, analyzing charged scalar fields in such geometry and how they can lead to growing modes in the regime of superradiant scattering.

The article is organized as follows. In section II the spherically symmetric charged black hole solution surrounded by an anisotropic fluid is presented and its features are discussed. In Section III we analyze the conditions for the superradiant scattering of charged scalar waves. Section IV is devoted to the quasinormal frequencies that can be obtained by means of analytical techniques, complemented by a numerical study in section V regarding quasinormal oscillations and instabilities. Our concluding remarks and final discussions are given in section VI.

II. BLACK HOLE SOLUTIONS

We consider a spherically symmetric solution describing black holes surrounded by anisotropic fluids [27],

$$ds^2 = -f(r)dt^2 + \frac{dr^2}{f(r)} + r^2(d\theta^2 + \sin^2\theta d\phi^2), \quad (1)$$

with

$$f(r) = 1 - \frac{2M}{r} + \frac{Q^2}{r^2} - \frac{c}{r^\sigma}, \quad (2)$$

where M represents the black hole mass, Q its electric charge, c is a dimensional normalization constant, and $\sigma = 3\omega_f + 1$, being ω_f a parameter characterizing the anisotropic fluid, which obeys the equation of state $p_f = \omega_f \rho_f$.

Notice that some classical solutions can be recovered for certain values of ω_f as follows. For $\omega_f = -1$ we have a Reissner-Nordström-(Anti)-de Sitter black hole where $3c$ plays the role of the cosmological constant. Moreover, for $\omega_f = -1/3$ we recover a topological Reissner-Nordström solution, while in case $\omega_f = 1/3$, we have the Reissner-Nordström metric with a shifted charge provided that $c < Q^2$. Also for $Q = 0$ and $\omega_f = 0$ we have a Schwarzschild spacetime with mass parameter $2M + c$.

In this work we will consider several cases where $c > 0$ and $-2 \leq \sigma \leq 1$ ($-1 \leq \omega_f \leq 0$) in order to fulfill the null energy condition [34, 35]. For this range of values the solutions (2) display a causal structure which is very similar to the Reissner-Nordström-de Sitter black hole, except for the light-like structure beyond the cosmological-like horizon ($r > r_c$) [33].

When considering the roots of the polynomial (2), we have three different horizons: r_i (inner/Cauchy), r_h (event), and r_c (cosmological-like), ordered according to $r_i < r_h < r_c$. The observable universe where the probe field is analyzed is contained in the region $r_h \leq r \leq r_c$.

In the next section we examine a charged scalar perturbation in this background and derive the necessary condition in order to obtain superradiant modes.

III. SUPERRADIANCE CONDITION

Let us consider a charged scalar field perturbation Ψ obeying the Klein-Gordon equation,

$$[(\nabla^\nu - iqA^\nu)(\nabla_\nu - iqA_\nu) - \mu^2]\Psi = 0, \quad (3)$$

where μ and q are the mass and charge of the field Ψ and $A_\mu = -\delta_\mu^0 Q/r = \delta_\mu^0 \Phi$ is the black hole electromagnetic potential.

We will use a spherically symmetric general Ansatz given by

$$ds^2 = -f(r)dt^2 + \frac{dr^2}{f(r)} + r^2(d\theta^2 + \sin^2 \theta d\phi^2), \quad (4)$$

and the following decomposition for the scalar field, $\Psi(t, r, \theta, \phi) = e^{-i\omega t}R(r)e^{im\phi}S(\theta)$, with $S(\theta) = P_\ell^m(\cos \theta)$ being the associated Legendre polynomials. In this way the radial part of

Eq.(3) becomes,

$$f^2 \frac{d^2 R}{dr^2} + \left(\frac{2f^2}{r} + f f' \right) \frac{dR}{dr} + \left[\omega^2 + 2q\omega\Phi + q^2\Phi^2 - \mu^2 f - \ell(\ell+1) \frac{f}{r^2} \right] R = 0. \quad (5)$$

By defining $\Delta_r = r^2 f(r)$ and in terms of the black hole charge this equation can be rewritten as,

$$\Delta_r \frac{d}{dr} \left(\Delta_r \frac{dR}{dr} \right) + \left\{ (\omega r^2 - qQr)^2 - \Delta_r [\ell(\ell+1) + \mu^2 r^2] \right\} R = 0. \quad (6)$$

In terms of the tortoise coordinate defined as

$$r_* = \int \frac{dr}{f(r)}, \quad (7)$$

and with $R(r) = \frac{X(r)}{r}$, Eq.(6) turns to be

$$\frac{d^2 X}{dr_*^2} + \Theta X = 0, \quad (8)$$

where the potential can be written as

$$\Theta = \left(\omega - \frac{qQ}{r} \right)^2 - \frac{\Delta_r}{r^2} \left[\frac{\ell(\ell+1)}{r^2} + \mu^2 + \left(\frac{\Delta'_r}{r^3} - \frac{2\Delta_r}{r^4} \right) \right]. \quad (9)$$

Let us check the scalar field behavior near the horizons. Near the event horizon $r \rightarrow r_h$ we have $\Delta_r \rightarrow 0$ and from Eq.(9) we see that

$$\Theta \rightarrow \left(\omega - \frac{qQ}{r_h} \right)^2 = (\omega + q\Phi_h)^2. \quad (10)$$

Thus, the scalar field behaves as $e^{-i\omega t \pm i(\omega + q\Phi_h)r_*}$ with Φ_h the electromagnetic potential at the event horizon. Moreover, as there are only ingoing waves at the horizon (classically nothing comes out from r_h), we should choose the (-) sign.

In the neighborhood of the cosmological-like horizon $r \rightarrow r_c$, $\Delta_r \rightarrow 0$ and analogously to the previous case we have

$$\Theta \rightarrow (\omega + q\Phi_c)^2, \quad (11)$$

so that the scalar field behaves as $e^{-i\omega t \pm i(\omega + q\Phi_c)r_*}$ with Φ_c the electromagnetic potential at the cosmological-like horizon. Here we keep both signs since we can have ingoing and outgoing waves expressing the right superradiance boundary condition.

From these two kinds of asymptotic behavior we can write a solution for Eq.(8) as

$$X(r_*) = \begin{cases} \mathcal{T} e^{-i(\omega + q\Phi_h)r_*} & \text{as } r \rightarrow r_h \\ \mathcal{R} e^{i(\omega + q\Phi_c)r_*} + \mathcal{I} e^{-i(\omega + q\Phi_c)r_*} & \text{as } r \rightarrow r_c \end{cases}, \quad (12)$$

where we have labelled \mathcal{I} , \mathcal{R} , and \mathcal{T} as the incident, reflected, and transmitted wave amplitudes, respectively. We emphasize that in such scattering, different from a quasinormal mode, ω represents the frequency of the scattered wave and is a real number.

Using the fact that the Wronskian of the solutions, $W = X\partial_{r_*}X^* - X^*\partial_{r_*}X$, must be conserved we find that

$$|\mathcal{R}|^2 = |\mathcal{I}|^2 - \frac{\kappa}{\lambda}|\mathcal{T}|^2, \quad (13)$$

where $\kappa = \omega + q\Phi_h$ and $\lambda = \omega + q\Phi_c$. Thus, in order to have superradiance we should have $\kappa/\lambda < 0$, so that

$$\frac{qQ}{r_c} < \omega < \frac{qQ}{r_h}. \quad (14)$$

We see that this condition is the same as that for a Reissner-Nordström-de Sitter black hole [36, 37] with the difference that now the position of the cosmological-like horizon depends on the anisotropic fluid parameters.

In the next section we will discuss the quasinormal behavior of the solutions of the radial equation (6) for some particular cases which can be solved analytically.

IV. ANALYTICAL QUASINORMAL FREQUENCIES

We will consider two cases where the quasinormal frequencies can be extracted in an analytical way by means of a suitable method. The first represents a family of QNMs controlling the field evolution near the cosmological-like horizon. The latter brings near-extremal modes (highest cosmological term) appearing in the spectra of the massive scalar field (absent in the massless case).

A. Cosmological-like frequencies

Now let us consider the behavior of the radial equation (6) far from the black hole, *i.e.*, $r - r_h \gg M$. In this case the black hole mass and charge can be neglected such that

$$\Delta_r \sim r^2(1 - cr^{-\sigma}). \quad (15)$$

This form is valid for $\sigma < 0$, when a cosmological-like horizon exists. The cases $0 \leq \sigma \leq 1$ correspond to asymptotically flat black holes which are out of the scope of this paper. Thus,

Eq.(6) can be written as

$$(1 - cr^{-\sigma}) \frac{d^2R}{dr^2} + \left[\frac{2}{r} - \frac{c(2 - \sigma)}{r^{1+\sigma}} \right] \frac{dR}{dr} + \left[\frac{\omega^2}{1 - cr^{-\sigma}} - \frac{\ell(\ell + 1)}{r^2} - \mu^2 \right] R = 0. \quad (16)$$

Let us make a change of variable, $y = 1 - cr^{-\sigma}$, such that Eq.(16) takes the form,

$$y(1 - y)^{2+2/\sigma} \frac{d^2R}{dy^2} + \left\{ \left[\frac{2}{\sigma} - \left(1 + \frac{1}{\sigma} \right) y \right] (1 - y)^{1+2/\sigma} - \frac{(2 - \sigma)}{\sigma} (1 - y)^{2+2/\sigma} \right\} \frac{dR}{dy} + \left[\frac{\bar{\omega}^2}{y} - \frac{\ell(\ell + 1)}{\sigma^2} (1 - y)^{2/\sigma} - \bar{\mu}^2 \right] R = 0, \quad (17)$$

where $\bar{\omega}^2 = \frac{c^{2/\sigma} \omega^2}{\sigma^2}$ and $\bar{\mu}^2 = \frac{c^{2/\sigma} \mu^2}{\sigma^2}$.

Furthermore, we use the following Ansatz, $R(y) = y^{\frac{-i\omega c^{1/\sigma}}{\sigma}} (1 - y)^{-\ell/\sigma} G(y)$, such that from Eq.(17) we obtain a new equation for $G(y)$,

$$y(1 - y)^{2+2/\sigma} \frac{d^2G}{dy^2} + \left[(1 - 2i\bar{\omega}) (1 - y)^{2+2/\sigma} + (2\ell + 1 - \sigma) \frac{y}{\sigma} (1 - y)^{1+2/\sigma} \right] \frac{dG}{dy} + \left\{ \frac{\bar{\omega}^2}{y} [1 - (1 - y)^{2+2/\sigma}] - \frac{i\bar{\omega}}{\sigma} (2\ell + 1 - \sigma) (1 - y)^{1+2/\sigma} - \frac{\ell}{\sigma^2} (\ell + 1 - \sigma) (1 - y)^{1+2/\sigma} - \bar{\mu}^2 \right\} G = 0. \quad (18)$$

In what follows we will consider some specific cases.

1. Case $\sigma = -2$

In this case the metric (2) turns out to be the Reissner-Nordström-de Sitter black hole.

Thus, Eq.(18) becomes

$$y(1 - y) \frac{d^2G}{dy^2} + \left[1 + \frac{i\omega}{\sqrt{c}} - \left(\ell + \frac{5}{2} + \frac{i\omega}{\sqrt{c}} \right) y \right] \frac{dG}{dy} + \left[\frac{\omega^2 - \mu^2}{4c} - \frac{i\omega}{2\sqrt{c}} \left(\ell + \frac{3}{2} \right) - \frac{\ell}{4} (\ell + 3) \right] G = 0, \quad (19)$$

whose solution can be written in terms of hypergeometric functions so that the solution to Eq.(17) turns to be

$$R(y) = (1 - y)^{\ell/2} \left[A y^{\frac{i\omega}{2\sqrt{c}}} {}_2F_1(\alpha_1, \beta_1; \gamma_1; y) + B y^{\frac{-i\omega}{2\sqrt{c}}} {}_2F_1(\alpha_2, \beta_2; \gamma_2; y) \right], \quad (20)$$

with A and B being constant amplitudes and

$$\begin{aligned} \alpha_1 &= \frac{3}{4} + \frac{\ell}{2} + \frac{\sqrt{9c - 4\mu^2}}{4\sqrt{c}} + \frac{i\omega}{2\sqrt{c}}, & \alpha_2 &= \alpha_1^* \\ \beta_1 &= \frac{3}{4} + \frac{\ell}{2} - \frac{\sqrt{9c - 4\mu^2}}{4\sqrt{c}} + \frac{i\omega}{2\sqrt{c}}, & \beta_2 &= \beta_1^* \\ \gamma_1 &= 1 + \frac{i\omega}{\sqrt{c}}, & \gamma_2 &= \gamma_1^*. \end{aligned} \quad (21)$$

Since this result comes from an equation originally developed for a black hole background, it displays an incident wave and a reflected wave. However, as we are in a region close to the cosmological-like horizon and we have neglected the influence of the black hole, we can take the incident wave only and obtain a solution for a de Sitter geometry. Moreover, we can rewrite our solution using the following transformation for the hypergeometric function [38],

$$\begin{aligned} {}_2F_1(a, b; c; z) &= \frac{\Gamma(c)\Gamma(c-a-b)}{\Gamma(c-a)\Gamma(c-b)} {}_2F_1(a, b; a+b-c+1; 1-z) \\ &+ (1-z)^{c-a-b} \frac{\Gamma(c)\Gamma(a+b-c)}{\Gamma(a)\Gamma(b)} {}_2F_1(c-a, c-b; c-a-b+1; 1-z), \end{aligned} \quad (22)$$

and take the limit $y \rightarrow 1$, which corresponds to small r , to obtain the following result,

$$R(r) \sim B \Gamma\left(1 - \frac{i\omega}{\sqrt{c}}\right) \left[\frac{c^{\ell/2} \Gamma\left(-\frac{1}{2} - \ell\right) r^\ell}{\Gamma\left(\frac{1}{4} - \frac{\ell}{2} - \frac{\sqrt{9c-4\mu^2}}{4\sqrt{c}} - \frac{i\omega}{2\sqrt{c}}\right) \Gamma\left(\frac{1}{4} - \frac{\ell}{2} + \frac{\sqrt{9c-4\mu^2}}{4\sqrt{c}} - \frac{i\omega}{2\sqrt{c}}\right)} \right. \\ \left. + \frac{c^{-(\ell+1)/2} \Gamma\left(\frac{1}{2} + \ell\right) r^{-\ell-1}}{\Gamma\left(\frac{3}{4} + \frac{\ell}{2} + \frac{\sqrt{9c-4\mu^2}}{4\sqrt{c}} - \frac{i\omega}{2\sqrt{c}}\right) \Gamma\left(\frac{3}{4} + \frac{\ell}{2} - \frac{\sqrt{9c-4\mu^2}}{4\sqrt{c}} - \frac{i\omega}{2\sqrt{c}}\right)} \right]. \quad (23)$$

This solution diverges when $r \rightarrow 0$ due to the term $r^{-\ell-1}$. Thus, in order to obtain a regular solution we impose that any of the Γ -functions in the denominator of this term should go to infinity, *i.e.*, the argument of the Γ -function must be a negative integer N . In this way we obtain a set of frequencies for de Sitter solution,

$$\omega = -i\sqrt{c} \left(2N + \ell + \frac{3}{2} \mp \frac{\sqrt{9c-4\mu^2}}{2\sqrt{c}} \right). \quad (24)$$

The \mp signs correspond to the first or second choice of Γ -function, respectively. The $(-)$ choice agrees with the quasinormal frequencies for pure de Sitter spacetime obtained in [39]. We see that if $\mu = 0$, ω is always imaginary and negative, what assures the stability of this geometry. Conversely, if $\mu \neq 0$, ω can have a real part provided that $\mu^2 > 9c/4$.

2. Case $\sigma = -1$

In this case we have a metric describing a charged black hole surrounded by an anisotropic fluid with state parameter $\omega_f = -2/3$. Thus, Eq.(18) becomes

$$y \frac{d^2G}{dy^2} + \left[1 + \frac{2i\omega}{c} - \frac{2(\ell+1)y}{1-y} \right] \frac{dG}{dy} - \left[\frac{2i\omega(\ell+1)}{c(1-y)} + \frac{\ell(2+\ell)}{1-y} + \frac{\mu^2}{c^2} \right] G = 0. \quad (25)$$

Let us divide our study here in two cases, massless and massive perturbations. For a massless perturbation ($\mu = 0$) the solution of Eq.(25) is expressed in terms of hypergeometric functions so that the complete solution to Eq.(17) is given by

$$R(y) = (1 - y)^\ell \left[A y^{\frac{i\omega}{c}} {}_2F_1(\alpha_3, \beta_3; \gamma_3; y) + B y^{-\frac{i\omega}{c}} {}_2F_1(\alpha_4, \beta_4; \gamma_4; y) \right], \quad (26)$$

where A and B are constant amplitudes and

$$\begin{aligned} \alpha_3 &= 1 + \ell - \sqrt{1 - \frac{\omega^2}{c^2}} + \frac{i\omega}{c}, & \alpha_4 &= \alpha_3^* \\ \beta_3 &= 1 + \ell + \sqrt{1 - \frac{\omega^2}{c^2}} + \frac{i\omega}{c}, & \beta_4 &= \beta_3^* \\ \gamma_3 &= 1 + \frac{2i\omega}{c}, & \gamma_4 &= \gamma_3^*. \end{aligned} \quad (27)$$

Analogously to the case $\sigma = -2$ we only take the incident wave and find the small r limit by applying the transformation in Eq.(22) and taking the limit $y \rightarrow 1$ to finally obtain,

$$\begin{aligned} R(r) \sim & B \Gamma \left(1 - \frac{2i\omega}{c} \right) \left[\frac{c^\ell \Gamma(-1 - 2\ell) r^\ell}{\Gamma \left(-\ell + \sqrt{1 - \frac{\omega^2}{c^2}} - \frac{i\omega}{c} \right) \Gamma \left(-\ell - \sqrt{1 - \frac{\omega^2}{c^2}} - \frac{i\omega}{c} \right)} \right. \\ & \left. + \frac{c^{-1-\ell} \Gamma(1 + 2\ell) r^{-1-\ell}}{\Gamma \left(1 + \ell - \sqrt{1 - \frac{\omega^2}{c^2}} - \frac{i\omega}{c} \right) \Gamma \left(1 + \ell + \sqrt{1 - \frac{\omega^2}{c^2}} - \frac{i\omega}{c} \right)} \right]. \end{aligned} \quad (28)$$

As the second term of this solution diverges as $r \rightarrow 0$, we demand that any of the Γ -functions in the denominator of this term should go to infinity. In fact, both Γ -functions lead to only one solution for the quasinormal frequencies for this spacetime,

$$\omega = -\frac{ic}{2} \frac{(N + \ell + 2)(N + \ell)}{N + \ell + 1}, \quad (29)$$

where N is an integer number. Unlike de Sitter case, the frequency here has no chance of having a real part, it is purely imaginary and, in addition, always stable since ω is negative for any choice of parameters.

Now let us turn our attention to the massive perturbation case. Eq.(25) has a solution in terms of the confluent Heun functions and thus, the complete solution to Eq.(17) turns to be

$$R(y) = (1 - y)^\ell \left[C_1 y^{\frac{i\omega}{c}} \text{HeunC}(0, \alpha_5, \beta_5, \gamma_5, \eta_5, y) + C_2 y^{-\frac{i\omega}{c}} \text{HeunC}(0, -\alpha_5, \beta_5, \gamma_5, \eta_5, y) \right], \quad (30)$$

where C_1 and C_2 are constant amplitudes and the Heun functions parameters are given by

$$\begin{aligned}\alpha_5 &= \frac{2i\omega}{c} \\ \beta_5 &= 2\ell + 1 \\ \gamma_5 &= -\frac{\mu^2}{c^2} \\ \eta_5 &= \ell^2 + \ell - \frac{1}{2} + \frac{\mu^2}{c^2}.\end{aligned}\tag{31}$$

In order to find the small r limit, *i.e.*, $y \rightarrow 1$, we will use the following connection formula [40–42]

$$\begin{aligned}\text{HeunC}(0, b, k, d, e, z) &= \frac{a_1 \Gamma(b+1) \Gamma(-k)}{\Gamma(1-k+\zeta) \Gamma(b-\zeta)} \text{HeunC}(0, k, b, -d, e+d, 1-z) \\ &\quad + \frac{a_2 \Gamma(b+1) \Gamma(k)}{\Gamma(1+k+\lambda) \Gamma(b-\lambda)} (1-z)^{-k} \text{HeunC}(0, -k, b, -d, e+d, 1-z),\end{aligned}\tag{32}$$

with a_1 and a_2 arbitrary constants and ζ and λ being the solution of the following equations,

$$\begin{aligned}\zeta^2 + (1-b-k)\zeta - \epsilon - b - k + \frac{d}{2} &= 0 \\ \lambda^2 + (1-b+k)\lambda - \epsilon - b(k+1) + \frac{d}{2} &= 0 \\ \epsilon &= \frac{1}{2}[1 - (b+1)(k+1)] - e.\end{aligned}\tag{33}$$

By taking only the incident wave as before the limit $y \rightarrow 1$ gives

$$\begin{aligned}R(r) &\sim \frac{D_1 c^\ell \Gamma(1 - \frac{2i\omega}{c}) \Gamma(-2\ell - 1) r^\ell}{\Gamma\left(-\frac{i\omega}{c} - \ell + \sqrt{1 - \frac{\mu^2}{2c^2} - \frac{\omega^2}{c^2}}\right) \Gamma\left(-\frac{i\omega}{c} - \ell - \sqrt{1 - \frac{\mu^2}{2c^2} - \frac{\omega^2}{c^2}}\right)} \\ &\quad + \frac{D_2 c^{-1-\ell} \Gamma(1 - \frac{2i\omega}{c}) \Gamma(2\ell + 1) r^{-1-\ell}}{\Gamma\left(-\frac{i\omega}{c} + \ell + 1 + \sqrt{1 - \frac{\mu^2}{2c^2} - \frac{\omega^2}{c^2}}\right) \Gamma\left(-\frac{i\omega}{c} + \ell + 1 - \sqrt{1 - \frac{\mu^2}{2c^2} - \frac{\omega^2}{c^2}}\right)},\end{aligned}\tag{34}$$

with D_1 and D_2 constants. As the second term in Eq.(34) diverges when $r \rightarrow 0$, we need to impose that any of the Γ functions must go to infinity, both choices drive us to the same result,

$$\omega = -\frac{ic}{2(N+\ell+1)} \left[(N+\ell+2)(N+\ell) + \frac{\mu^2}{2c^2} \right].\tag{35}$$

By comparing with Eq.(29) we see that the perturbation mass makes the frequency more negative, thus, the background keeps its stability.

3. Case $\sigma = -1/2$

In this case the metric depicts a charged black hole surrounded by an anisotropic fluid with state parameter $\omega = -1/2$ and Eq.(18) takes the form,

$$\frac{y}{(1-y)^2} \frac{d^2G}{dy^2} + \left[\frac{1-4(\ell+1)y}{(1-y)^3} + \frac{4i\omega}{(1-y)^2c^2} \right] \frac{dG}{dy} - \left[\frac{2\ell(2\ell+3)}{(1-y)^3} + \frac{2i\omega(4\ell+3)}{(1-y)^3c^2} \right. \\ \left. + \frac{4\omega^2(2-y)}{(1-y)^2c^4} + \frac{4\mu^2}{c^4} \right] G = 0. \quad (36)$$

Only the massless case has analytical solution so that the solution of Eq.(17) is given in terms of the confluent Heun functions as

$$R(y) = (1-y)^{2\ell} e^{\frac{2i\omega y}{c^2}} \left[C_3 y^{\frac{2i\omega}{c^2}} \text{HeunC}(\alpha_6, \beta_6, \gamma_6, \eta_6, \nu_6, y) \right. \\ \left. + C_4 y^{-\frac{2i\omega}{c^2}} \text{HeunC}(\alpha_6, -\beta_6, \gamma_6, \eta_6, \nu_6, y) \right], \quad (37)$$

with C_3 and C_4 arbitrary constants and the parameters of the Heun functions are written as

$$\alpha_6 = \frac{4i\omega}{c^2} = \beta_6 \\ \gamma_6 = 2 + 4\ell \\ \eta_6 = -\frac{8\omega^2}{c^4} \\ \nu_6 = 4\ell^2 + 4\ell - 1 + \frac{8\omega^2}{c^4}. \quad (38)$$

In order to find the small r limit ($y \rightarrow 1$) we should use a connection formula analogous to Eq.(32), that could lead to impose some condition on the Γ functions probably appearing there and thus extract the frequencies. However, this formula does not exist yet as far as we know.

Summarizing the main results of this subsection, the superradiance in cosmological QNMs can be triggered for the case $\omega_f = -1$ whenever $\mu > 3\sqrt{c}/2$, if the real part of the mode frequency belongs to the interval (14), rendering a stable evolution. Such a situation characterizes a fundamental distinction between superradiance and instability. The first do not imply the second, the reciprocal being true. The cosmological frequencies for $\omega_f = -2/3$, on the other hand, do not cause the same phenomenon since the frequencies are purely imaginary.

B. Near-extremal frequencies

It is useful to mention that the near-extremal case for the asymptotically flat RN black hole with high values of Q was discussed in [43], where near-extremal regime means that the Cauchy and the event horizons are close enough. The frequencies displayed in relation (39) of this reference are also present in the RNdS black hole [44], taking control over the field profile evolution in the very high charge regime. The same behavior is expected for the black hole we present in this paper showing no new physics, thus, this case will not be analyzed here. Instead, we will turn our attention to the other possible near-extremal case, *i.e.*, when the event and cosmological-like horizons are nearby.

In order to illustrate this regime we will choose $\sigma = -1$ ($\omega_f = -2/3$) such that the metric coefficient (2) becomes

$$f(r) = 1 - \frac{2M}{r} + \frac{Q^2}{r^2} - c r, \quad (39)$$

which can also be written in terms of its horizons as [33]

$$f(r) = -\frac{c}{r^2}(r - r_c)(r - r_h)(r - r_i). \quad (40)$$

Here we stress that we will consider the regime where

$$\frac{r_c - r_h}{r_h - r_i} \ll 1, \quad (41)$$

i.e., when the cosmological-like and the event horizons are very close to each other. As the physical region of interest lies between r_h and r_c , we can write Eq.(40) in an approximate form,

$$f(r) \approx 2\kappa_h \frac{(r - r_h)(r_c - r)}{r_c - r_h}. \quad (42)$$

Here the surface gravity calculated at the event horizon, $\kappa_h = \frac{1}{2}f'(r)|_{r=r_h}$, in the same near-extremal regime, can be reduced to

$$\kappa_h \approx \frac{(r_c - r_h)}{4r_h^2} \left[1 - 3 \left(\frac{Q}{r_h} \right)^2 \right]. \quad (43)$$

In this limit we can also integrate Eq.(7) to have a relation between the radial and the tortoise coordinates,

$$r = \frac{r_c e^{2\kappa_h r_*} + r_h}{1 + e^{2\kappa_h r_*}}, \quad (44)$$

which is the same expression found in the near-extremal Reissner-Nordström-de Sitter black hole [45, 46]. Thus, in terms of the tortoise coordinate Eq.(42) turns out to be

$$f(r_*) \approx \frac{\kappa_h(r_c - r_h)}{2 \cosh^2(\kappa_h r_*)}. \quad (45)$$

As we will see in what follows, it is possible to find an analytical quasinormal spectrum for the near-extremal black hole considered here in the dimensionless large-mass regime, $\mu r_h \gg \max\{\kappa_h r_h, \ell(\ell + 1)\}$. We will use two different methods in order to attain this aim.

1. WKB method

In this case the potential (9) in terms of $f(r)$ can be approximated as

$$V(r) \approx \left(\omega - \frac{qQ}{r} \right)^2 - \mu^2 f(r). \quad (46)$$

So that we can use the WKB approximation [47] to extract the frequencies through the following equation,

$$\frac{i V(r_*^o)}{\sqrt{2 V''(r_*^o)}} = n + \frac{1}{2}; \quad n = 0, 1, 2, \dots \quad (47)$$

where $V'' = \frac{d^2 V}{dr_*^2}$ and $r_*^o(r_0)$ is the extremum point where $V'(r_*^o) = 0$, which yields

$$\omega - \frac{qQ}{r_0} = \frac{\mu^2 f'(r_*^o) r_0^2}{2qQ f(r_*^o)}. \quad (48)$$

In this expression again a prime ('') represents a derivative with respect to the tortoise coordinate. Thus, using the potential (46) the condition in Eq.(47) becomes

$$\frac{\left(\omega - \frac{qQ}{r_0} \right)^2 - \mu^2 f(r_*^o)}{\sqrt{\left[4 \left(\frac{qQ}{r_0^2} \right)^2 - 8 \left(\omega - \frac{qQ}{r_0} \right) \frac{qQ}{r_0^3} \right] f^2(r_*^o) + 4 \left(\omega - \frac{qQ}{r_0} \right) \frac{qQ}{r_0^2} f'(r_*^o) - 2\mu^2 f''(r_*^o)}} = -i \left(n + \frac{1}{2} \right). \quad (49)$$

As pointed out in [46] the large-mass regime also implies that $\omega_R \gg \omega_I$. Thus, by writing $\omega = \omega_R - i\omega_I$ in Eq.(49) it is possible to decouple the real part,

$$\left(\omega_R - \frac{qQ}{r_0} \right)^2 - \mu^2 f(r_*^o) = 0, \quad (50)$$

and the imaginary part of the near-extremal frequency,

$$\omega_I = \frac{1}{2} \left(n + \frac{1}{2} \right) \left(\omega_R - \frac{qQ}{r_0} \right)^{-1} \times \sqrt{\left[4 \left(\frac{qQ}{r_0^2} \right)^2 - 8 \left(\omega_R - \frac{qQ}{r_0} \right) \frac{qQ}{r_0^3} \right] f^2(r_*^o) + 4 \left(\omega_R - \frac{qQ}{r_0} \right) \frac{qQ}{r_0^2} f'(r_*^o) - 2\mu^2 f''(r_*^o)} . \quad (51)$$

In order to simplify Eq.(50) we notice that we can obtain a useful expression combining (48) and (50) so that

$$\frac{f'(r_*^o)}{f^{3/2}(r_*^o)} = \pm \frac{2qQ}{\mu r_0^2} \approx \pm \frac{2qQ}{\mu r_h^2} , \quad (52)$$

in which the last approximation will be explained more clearly in a subsequent paragraph. Moreover, if we use Eq.(45) in the last expression, it becomes

$$- \frac{\sqrt{\kappa_h} \sqrt{2} \sinh(\kappa_h r_*^o)}{\sqrt{r_c - r_h}} = \pm \frac{qQ}{\mu r_h^2} . \quad (53)$$

Furthermore, we use Eq.(43) to eliminate r_c , thus obtaining

$$\sinh(\kappa_h r_*^o) \approx \mp \sqrt{2} \frac{qQ}{\mu r_h} \left[1 - 3 \left(\frac{Q}{r_h} \right)^2 \right]^{-1/2} . \quad (54)$$

Now, let us return to the approximation made in Eq.(52). Combining (43) and (44) we can obtain

$$\frac{r_0}{r_h} = 1 + \frac{4\kappa_h r_h}{[1 - 3(Q/r_h)^2](1 - e^{-2\kappa_h r_*^o})} . \quad (55)$$

At this point we can use the following identity in the denominator of this expression,

$$\frac{2}{1 + e^{-2\alpha}} = 1 + \tanh \alpha = 1 + \frac{1}{\sqrt{1 + \frac{1}{\sinh^2 \alpha}}} , \quad (56)$$

then, we have

$$\frac{r_0}{r_h} = 1 + \frac{2\kappa_h r_h}{[1 - 3(Q/r_h)^2]} \left\{ 1 + \frac{1}{\sqrt{1 + \frac{[1-3(Q/r_h)^2](\mu r_h)^2}{2(qQ)^2}}} \right\} . \quad (57)$$

Therefore, to leading order $r_0 \approx r_h$ as we had employed before.

Finally, we can use (43) and (54) in (50) in order to obtain the real part of the near-extremal frequency,

$$\omega_R \approx \frac{qQ}{r_h} \pm \frac{\sqrt{2} \mu \kappa_h r_h}{\sqrt{1 - 3(Q/r_h)^2 + 2(qQ/\mu r_h)^2}} . \quad (58)$$

Although the (-) branch of this frequency appears to be below the upper limit in Eq.(14), *i.e.*, $\omega_R^- < qQ/r_h$, it does not mean that the quasinormal mode is necessarily superradiant. As pointed out in the *erratum* [48], due to the proximity of the horizons it is also true that $\omega_R^- < qQ/r_c$. However, we could also apply the same reasoning to $\omega_R^+ > qQ/r_c$. Therefore, due to the several approximations employed along the calculation and although the result offers a nice view of the qualitative behavior of this phenomenon, it does not seem possible to use quantitative arguments in order to conclude on the existence or not of superradiance in this near-extremal regime.

2. Pöschl-Teller potential

By taking into account the same approximation made in Eq.(46) for the near-extremal regime and using Eq.(45), we notice that Eq.(8) can be cast to

$$\frac{d^2X}{dr_*^2} + \left\{ \tilde{\omega}^2 - \frac{U_0}{\cosh^2[\alpha(r_* - r_*^m)]} \right\} X = 0, \quad (59)$$

which is a wave equation with a Pöschl-Teller potential (for a review on this equation check [49, 50]). The parameter r_*^m corresponds to the maximum of the potential obtained from $dU/dr_*|_{r_*^m} = 0$, U_0 is the value of the Pöschl-Teller potential at this point, $U_0 = U(r_*^m)$, and α is written in terms of the second derivative of the potential as $\alpha^2 = -(2U_0)^{-1}d^2U/dr_*^2|_{r_*^m}$. Thus, in our case the Pöschl-Teller potential is given by

$$U(r_*) = \frac{\mu^2 \kappa_h (r_c - r_h)}{2 \cosh^2(\kappa_h r_*)} = \frac{U_0}{\cosh^2(\kappa_h r_*)}, \quad (60)$$

whose maximum occurs at $r_*^m = 0$. In addition, the second derivative of the potential yields $\alpha = \pm \kappa_h$. Moreover, we set $\tilde{\omega} = \omega - qQ/r_0^m$ with r_0^m being the maximum in terms of the r coordinate. As the radial and tortoise coordinates are related by Eq.(44) and we are in the near-extremal regime, we find that

$$r_0^m = \frac{r_c + r_h}{2} \approx r_h. \quad (61)$$

Now, following the method described in [50] the quasi-normal frequencies extracted from the Pöschl-Teller potential are given by

$$\tilde{\omega} = \pm \sqrt{U_0 - \frac{\alpha^2}{4}} - i\alpha \left(n + \frac{1}{2} \right), \quad n = 0, 1, 2, \dots \quad (62)$$

Then, using Eq.(60) and Eq.(43) we can finally obtain

$$\omega = \frac{qQ}{r_h} \pm \frac{\kappa_h}{2} \sqrt{\frac{8\mu^2 r_h^2 - [1 - 3(Q/r_h)^2]}{1 - 3(Q/r_h)^2}} \mp i \kappa_h \left(n + \frac{1}{2} \right). \quad (63)$$

Now, if we compare both methods, something remarkable occurs. When we reduce the real part of both frequencies (58) and (63) by approximating their second terms in the large- μr_h limit, we obtain the same expression in both cases,

$$\omega_R \approx \frac{qQ}{r_h} \pm \frac{\sqrt{2} \mu \kappa_h r_h}{\sqrt{1 - 3(Q/r_h)^2}}. \quad (64)$$

This interesting result shows the validity of both methods in the near-extremal regime.

In the next section we will explore the general dynamical properties of the charged scalar field evolving in the black hole surrounded by an anisotropic fluid from a numerical point of view.

V. SCALAR FIELD DYNAMICS: FIELD PROFILE INSTABILITIES AND QUASI-NORMAL MODES

We now take into consideration the motion equation of the charged scalar field given by (3) with the line-element (1) written in double null coordinates,

$$ds^2 = -f dudv + r^2 d\Omega^2. \quad (65)$$

Then, the scalar equation takes the following form,

$$\left(\square - \mu^2 - q^2 A^2 - iq\nabla_\mu(g^{\mu\nu}A_\nu) - 2iqA_\mu g^{\mu\nu}\nabla_\nu \right) \Psi = 0, \quad (66)$$

which may be solved after choosing a gauge for the potential A . Usually papers discussing the scalar perturbation for RNdS black holes (see e. g. [17, 36, 37]) fixed the vector potential as $A_\mu dx^\mu = -\frac{Q}{r} dt$, which in double null coordinates turns to $-\frac{Q}{2r}(du + dv)$. Nevertheless, here we consider a different form of \mathbb{A} introduced in [51],

$$\mathbb{A}^\mu dx_\mu = A^\mu dx_\mu + d\lambda = -\frac{Q}{r} du \quad (67)$$

for the Maxwell potential. Clearly $d\lambda = \frac{Q}{r} dr_*$, where we recall the coordinate r_* introduced in (7). With a similar Ansatz of section III we decompose the field in terms of its angular and double-null coordinates,

$$\Psi = \frac{1}{r} \psi(u, v) Y_\ell^m(\theta, \phi), \quad (68)$$

such that the eigenvalue of the angular part of the field equation is the traditional $\ell(\ell + 1)$ depicted in equation (5). After some algebra the scalar equation can be written in the form,

$$\begin{aligned} & \frac{\ell(\ell + 1)f}{r^2}\psi + 4\partial_u\partial_v\psi + \frac{ff'}{r}\psi + \mu^2f\psi + if\frac{qQ(r_c + r_h)}{r^2(r_c - r_h)}\psi \\ & + 4i\frac{qQ}{r}\left(\frac{r_c - r}{r_c - r_h}\partial_u + \frac{r - r_h}{r_c - r_h}\partial_v\right)\psi + \frac{4q^2Q^2(r - r_c)(r - r_h)}{r^4(r_c - r_h)^2}\psi = 0, \end{aligned} \quad (69)$$

in which prime denotes derivative with respect to r . Equivalently we can put the equation into the form

$$\partial_u\partial_v\psi + \mathcal{P}_1\partial_u\psi + \mathcal{P}_2\partial_v\psi + \vartheta\psi = 0 \quad (70)$$

$$\mathcal{P}_1 = \frac{iqQ(r_c - r)}{r(r_c - r_h)}, \quad \mathcal{P}_2 = \frac{iqQ(r - r_h)}{r(r_c - r_h)} \quad (71)$$

$$\vartheta = \frac{q^2Q^2(r - r_c)(r - r_h)}{(r^2(r_c - r_h))^2} + \frac{f}{4r^2}\left(rf' + \mu^2r^2 + \ell(\ell + 1) + \frac{iqQ(r_c + r_h)}{r_c - r_h}\right) \quad (72)$$

which is the same as Eq.(18) of reference [51]. Now, in order to integrate the equation and obtain the field profile, we follow the same discretization scheme offered in [51]. In that case

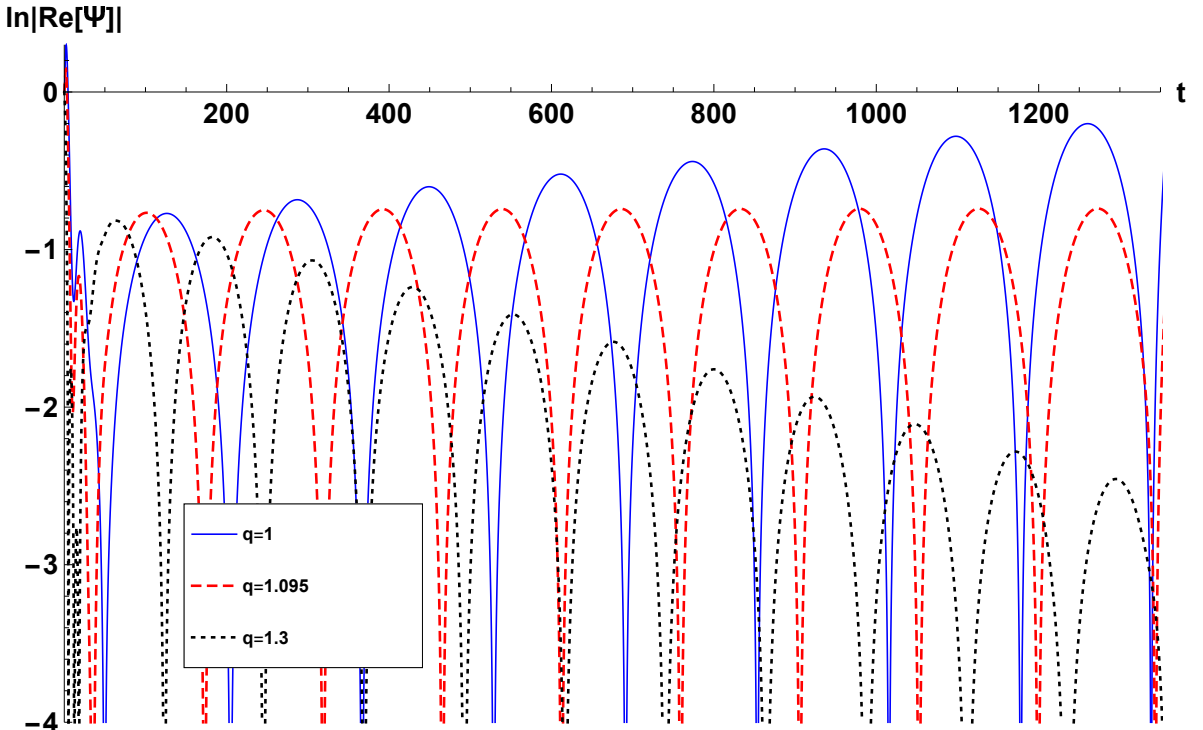


FIG. 1. Field profile evolution of the massless charged scalar field in a black hole background with $\omega_f = -2/3$. The parameters of the geometry read $M = 2Q = 1$ and $r_h/r_c = 0.06$.

the discretized field equation with grid h can be written as

$$\psi_N = \left(\frac{4}{h^2} + \frac{\mathcal{P}_{1S} + \mathcal{P}_{2S}}{2h} \right)^{-1} \left(4 \frac{\psi_E + \psi_W - \psi_S}{h^2} + \frac{\mathcal{P}_{1S} + \mathcal{P}_{2S}}{2h} \psi_S \right. \\ \left. - \frac{\mathcal{P}_{1S} - \mathcal{P}_{2S}}{2h} (\psi_E - \psi_W) - \frac{\vartheta_S}{2} (\psi_E + \psi_W) \right). \quad (73)$$

In the chargeless case ($\mathcal{P}_{1S} = \mathcal{P}_{2S} = 0$) Eq.(73) reduces to the usual equation for the anisotropic BH system with a massive scalar field evolving in the geometry (see *e.g.* [33]). The evolution scheme [52] considers a piece of a Cauchy surface that covers the physical universe in-between horizons [53] prescribed as

$$\psi(u_0, v) = \text{Exp}(-v^2), \quad \psi(u, v_0) = \text{Constant}. \quad (74)$$

The expected result is that of a field profile that decays in time encoding all the different families and overtones of quasinormal modes [44]. In the special case when $\ell = 0$ the superradiant instability described in the previous section turns the field profile evolution unstable. The emergence of this instability can be seen in Figure 1.

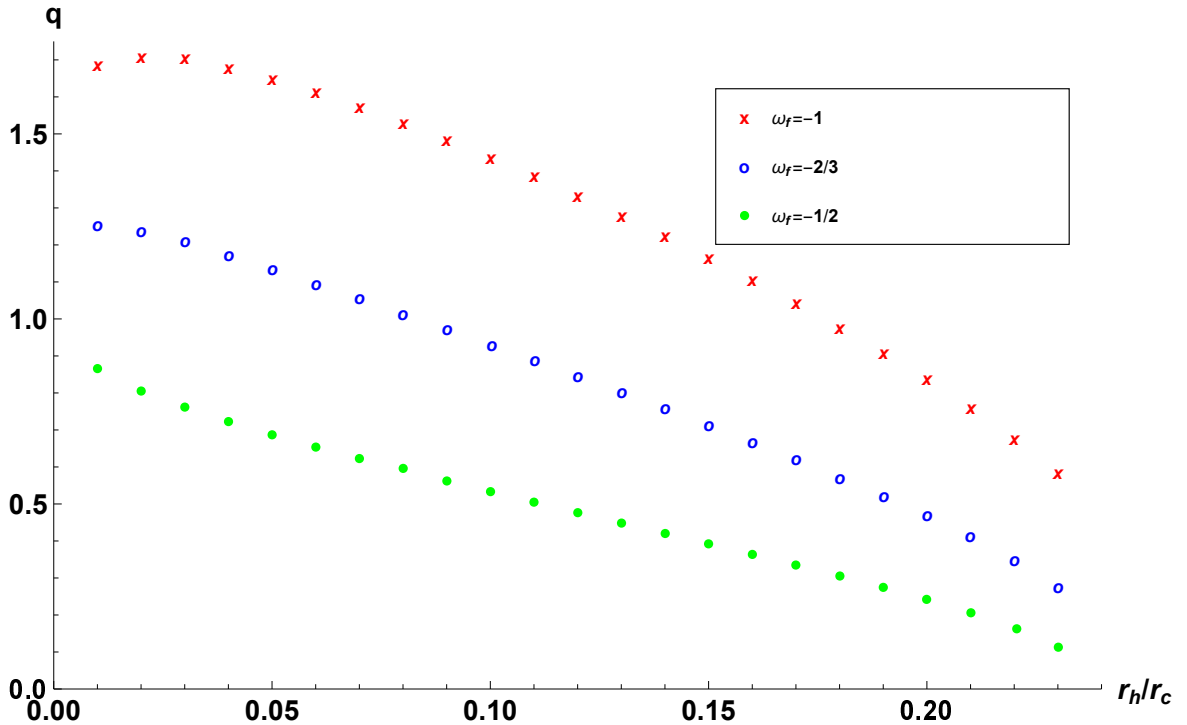


FIG. 2. Threshold of stability for the RN black hole with an anisotropic fluid perturbed by a charged massless scalar field. The geometry parameters read $M = 2Q = 1$. The points separate unstable perturbations (small charges) from stable ones (higher values of q).

TABLE I. The fundamental quasinormal mode or dominant unstable frequency for a charged massless scalar field ($\ell = 0$) propagating in black holes surrounded by different anisotropic fluids. The used parameters read $M = 2Q = q = 1$ and $r_h/r_c = n/50$.

n	$\omega_f = -1/2$	$\omega_f = -2/3$	$\omega_f = -1$
1	$0.0064389 - 0.00124552I$	$0.0068615 + 0.00067359I$	$0.0063505 + 0.00087822I$
2	$0.0106616 - 0.00224517I$	$0.0133091 + 0.00072804I$	$0.0128062 + 0.00134247I$
3	$0.0144385 - 0.00281848I$	$0.0193639 + 0.00049341I$	$0.0192766 + 0.00156047I$
4	$0.0184851 - 0.00295549I$	$0.0250369 + 0.00008897I$	$0.0257212 + 0.00158959I$
5	$0.0215718 - 0.00346489I$	$0.0305062 - 0.00043736I$	$0.0321117 + 0.00146573I$
6	$0.0245818 - 0.00368804I$	$0.0355059 - 0.00010150I$	$0.0384178 + 0.00121583I$
7	$0.0272386 - 0.00397286I$	$0.0402903 - 0.00016390I$	$0.0446355 + 0.00086085I$
8	$0.0299028 - 0.00422133I$	$0.0448270 - 0.00022836I$	$0.0507343 + 0.00041999I$
9	$0.0323380 - 0.00433221I$	$0.0491253 - 0.00293193I$	$0.0567144 - 0.00009158I$
10	$0.0344811 - 0.00452015I$	$0.0531979 - 0.00357178I$	$0.0625473 - 0.00065792I$

In this figure different field profiles are displayed for the same geometry parameters and different scalar field charges. In general, there is always a critical value of scalar charge up to which the superradiant modes are excited. In this case $q_c \sim 1.096$, such that whenever $q > 1.096$ only stable modes arise.

The evolution of the stable $l = 0$ modes (i. e. $q > q_c$) yields a dominant (longest-lived) quasinormal mode with $\Re(\omega) > 0$, thus acquiring a dynamical (oscillatory) behavior, what is different from the chargeless case in which purely imaginary frequencies dominate for small c [39, 54].

For the massless scalar field the cosmological modes do not foresee superradiant instabilities: condition (14) is not granted as long as all the modes are purely imaginary. The same can not be said for the massive field, superradiant excitations can occur for $\mu > \sqrt{3\Lambda/4}$ in the dS geometry (see Eq.(24)) for those modes.

A different portrait happens if we consider the photon sphere modes. Those can not be investigated analytically and numerical data is necessary (obtained using the steps showed above).

In Figure 2, we plot the threshold charge of a massless scalar field perturbing a RN

TABLE II. The fundamental quasinormal mode or dominant unstable frequency for a charged massless scalar field ($\ell = 0$) propagating in black holes surrounded by different anisotropic fluids. The used parameters read $\mathbf{n}/10 = M = 2Q = 1$.

q	$\omega_f = -1/2$	$\omega_f = -2/3$	$\omega_f = -1$
0.3	$0.0114059 - 0.00011398I$	$0.0155809 + 0.00014878I$	$0.0180741 + 0.00021956I$
0.4	$0.0153353 - 0.00051146I$	$0.0209804 + 0.00011015I$	$0.0242400 + 0.00032732I$
0.5	$0.0191454 - 0.00115331I$	$0.0264578 - 0.00007375I$	$0.0304947 + 0.00039823I$
0.6	$0.0227275 - 0.00197875I$	$0.0319610 - 0.00043600I$	$0.0368294 + 0.00040031I$
0.7	$0.0259926 - 0.00286929I$	$0.0374335 - 0.00098489I$	$0.0432262 + 0.00030828I$
0.8	$0.0289554 - 0.00363790I$	$0.0428236 - 0.00170890I$	$0.0496615 + 0.00010541I$
0.9	$0.0317541 - 0.00419641I$	$0.0480890 - 0.00258265I$	$0.0561100 - 0.00021642I$
1.0	$0.0344811 - 0.00452015I$	$0.0531979 - 0.00357178I$	$0.0625473 - 0.00065792I$
1.1	$0.0373037 - 0.00463810I$	$0.0581297 - 0.00463634I$	$0.0689514 - 0.00121401I$
1.2	$0.0402247 - 0.00472628I$	$0.0628750 - 0.00573345I$	$0.0753042 - 0.00187547I$
1.3	$0.0431738 - 0.00475754I$	$0.0674357 - 0.00681974I$	$0.0815912 - 0.00263045I$
1.4	$0.0462099 - 0.00477422I$	$0.0718256 - 0.00785421I$	$0.0878015 - 0.00346562I$
1.5	$0.0492465 - 0.00481309I$	$0.0760695 - 0.00880198I$	$0.0939276 - 0.00436711I$
1.6	$0.0523098 - 0.00481236I$	$0.0802012 - 0.00963880I$	$0.0999650 - 0.00532116I$

black hole with anisotropic fluid. As we can see, when the cosmological constant increases (or equivalently, the cosmological term), the range of instability decreases for every state parameter. In the same way, as we increase the state parameter, the range of instability diminishes.

We checked our recipes for the acquisition of the quasinormal frequencies and found that our results are in good agreement with the available literature of dS black holes. We tested our numerical code of characteristic integration together with the Prony method [52] obtaining the same results of Table one (first three overtones and unstable evolution) of reference [51] within a maximum discrepancy of 0.1%. In the quest of unstable/stable evolutions we also obtained the same threshold charge found in Table I of [37].

The quasinormal modes and unstable oscillations of spacetimes with different cosmological terms and fluid state parameter are listed in Table I.

As it was shown in Figure 2 for fixed M , Q , and c , there is always a critical q up which the field profile is dominated by an unstable oscillation. This is the reason why in Table I we can not see instabilities when $\omega_f = -1/2$ (those being present in the other cases). The presence of superradiant instabilities are enhanced with the increasing state parameter $|\omega_f|$.

A similar statement can be made if we observe Table II, where the fundamental quasi-normal modes for different values of scalar charge are displayed (and dominant unstable frequency when it is the case). As the charge of the scalar field increases, the spacetime response is given by stable profiles for every state parameter, although the smallest $|\omega_f|$ brought the least unstable fields.

VI. DISCUSSION AND FURTHER REMARKS

In this paper we studied the superradiant phenomenon in the background of a black hole surrounded by anisotropic fluids. By considering the charged version of the Klein-Gordon equation we derived the condition that a wave frequency should fulfill in order to generate superradiance. This condition turns out to be the same as in a RN-dS black hole, although now the position of the horizons depends on the fluid surrounding the black hole considered in this work. In addition, we should stress that in this context superradiance is a phenomenon of scattering waves with real frequencies.

Afterwards, we discussed the charged Klein-Gordon equation supplied by quasinormal boundary conditions. In this case we follow the same terminology as Ref. [37] and consider a quasinormal mode to be superradiant whenever the real part of its frequency satisfies Eq.(14). Firstly, we consider some special cases where an analytical solution is possible to obtain. These cases correspond to the cosmological-like frequencies, which are obtained in the small black hole mass and small black hole charge limits, and the near-extremal regime, where the event and cosmological-like horizons are nearby.

The cosmological-like case was discussed for massless and massive scalar perturbations in the background of a black hole surrounded by anisotropic fluids with state parameters $\omega_f = -1$ and $\omega_f = -2/3$. We showed that the frequency of the former case (RN-dS) can have a real part whenever $\mu > 3\sqrt{c}/2$ and if this real part falls in the superradiant interval given by Eq.(14), it can render superradiant quasinormal modes. Moreover, as we write the quasinormal frequency as $\omega = \omega_R - i\omega_I$, it is clear from Eq.(24) that the imaginary part is

positive, thus, the mode is stable. This result reinforces the fact that a superradiant mode is not necessarily unstable. On the other hand, the frequencies for the latter case $\omega_f = -2/3$ lack real part, therefore, superradiant modes are absent.

In the near-extremal regime we employed two methods, WKB and Pöschl-Teller potential, in order to get approximate expressions for the quasinormal frequencies. Our results show that superradiant modes are possible although it is not clear what combination of parameters could produce an exact value inside the superradiant regime. In fact, according to the condition given by Eq.(14), the superradiant interval for the quasinormal modes in the near-extremal regime seems to be tiny. In effect, our results (58) and (63) show frequencies whose real part could be superradiant, however, given the approximations made in the calculations it was not possible to give a definite answer on this possibility.

Subsequently, we addressed the dynamics of the charged scalar perturbation in a more general way from a numerical point of view. We considered an evolution scheme in double-null coordinates in our numerical code of characteristic integration together with the Prony method. Our numerical development gives rise to unstable profiles that comply with the superradiant QNM condition. Our results show that there exists a critical value of the scalar charge above which superradiant modes are excited. Above this critical value superradiant QNMs are stable showing again that superradiance does not imply instability. Furthermore, this threshold charge depends on the state parameter ω_f and the parameter c coming from the cosmological-like term. We found that the range of instability decreases when the cosmological-like constant increases, a fact that complies with the analytical result for the cosmological-like frequencies when the cosmological term is dominant. In addition, the higher the state parameter becomes, the shorter the range of instability turns. These results are in perfect agreement with Refs. [37, 51].

Finally, based in our analytical and numerical results we can conclude that superradiant phenomenon is present in black holes surrounded by anisotropic fluids. Further lines of investigation on this subject include more general cases of dirty black holes that could mimic more realistic astronomical situations.

ACKNOWLEDGMENTS

This work was partially supported by UFMT (*Universidade Federal de Mato Grosso*) under project PROPEQ-CAP-401/2019.

- [1] B. P. Abbott *et al.* (LIGO Scientific, Virgo), *Physical Review D* **93**, 122003 (2016).
- [2] K. Akiyama *et al.* (Event Horizon Telescope), *Astrophysical Journal Letters* **875**, L1 (2019).
- [3] The GRAVITY Collaboration, Abuter, R., *et al.*, *Astronomy & Astrophysics* **625**, L10 (2019).
- [4] V. Cardoso and P. Pani, *Nature Astronomy* **1**, 586 (2017).
- [5] T. Regge and J. A. Wheeler, *Physical Review* **108**, 1063 (1957).
- [6] G. T. Horowitz and V. E. Hubeny, *Physical Review D* **62**, 024027 (2000).
- [7] D. T. Son and A. O. Starinets, *Journal of High Energy Physics* **09**, 042 (2002).
- [8] A. Nunez and A. O. Starinets, *Physical Review D* **67**, 124013 (2003).
- [9] V. Cardoso, A. S. Miranda, E. Berti, H. Witek, and V. T. Zanchin, *Physical Review D* **79**, 064016 (2009).
- [10] K. Jusufi, *Physical Review D* **101**, 084055 (2020).
- [11] K. Jusufi, *Physical Review D* **101**, 124063 (2020).
- [12] B. Cuadros-Melgar, R. Fontana, and J. de Oliveira, *Physics Letters B* **811**, 135966 (2020).
- [13] E. Berti, V. Cardoso, and A. O. Starinets, *Classical and Quantum Gravity* **26**, 163001 (2009).
- [14] S. L. Detweiler, *Physical Review D* **22**, 2323 (1980).
- [15] Z. Zhu, S.-J. Zhang, C. E. Pellicer, B. Wang, and E. Abdalla, *Physical Review D* **90**, 044042 (2014), [Addendum: *Phys.Rev.D* 90, 049904 (2014)].
- [16] R. A. Konoplya and A. Zhidenko, *Physical Review D* **90**, 064048 (2014).
- [17] K. Destounis, *Physical Review D* **100**, 044054 (2019).
- [18] R. Brito, V. Cardoso, and P. Pani, *Lecture Notes in Physics* **906**, pp.1 (2015).
- [19] Y. B. Zel'Dovich, *Journal of Experimental and Theoretical Physics* **14**, 180 (1971).
- [20] Y. B. Zel'Dovich, *Soviet Journal of Experimental and Theoretical Physics* **35**, 1085 (1972).
- [21] J. M. Bardeen, W. H. Press, and S. A. Teukolsky, *Astrophysical Journal* **178**, 347 (1972).
- [22] J. D. Bekenstein, *Physical Review D* **7**, 949 (1973).
- [23] G. Denardo and R. Ruffini, *Physics Letters B* **45**, 259 (1973).

- [24] W. H. Press and S. A. Teukolsky, *Nature* **238**, 211 (1972).
- [25] V. Cardoso and O. J. C. Dias, *Physical Review D* **70**, 084011 (2004).
- [26] H. Furuhashi and Y. Nambu, *Progress of Theoretical and Experimental Physics* **112**, 983 (2004).
- [27] V. V. Kiselev, *Classical and Quantum Gravity* **20**, 1187 (2003).
- [28] J. de Oliveira and R. D. B. Fontana, *Physical Review D* **98**, 044005 (2018).
- [29] S.-b. Chen and J.-l. Jing, *Classical and Quantum Gravity* **22**, 4651 (2005).
- [30] C. Ma, Y. Gui, W. Wang, and F. Wang, *Central European Journal of Physics* **6**, 194 (2008).
- [31] Y. Zhang, Y. X. Gui, and F. Li, *General Relativity and Gravitation* **39**, 1003 (2007).
- [32] N. Varghese and V. C. Kuriakose, *Modern Physics Letters A* **29**, 1450113 (2014).
- [33] B. Cuadros-Melgar, R. D. B. Fontana, and J. de Oliveira, *The European Physical Journal C* **80**, 848 (2020).
- [34] M. Visser, *Classical and Quantum Gravity* **37**, 045001 (2020).
- [35] P. Boonserm, T. Ngampitipan, A. Simpson, and M. Visser, *Physical Review D* **101**, 024022 (2020).
- [36] Z. Zhu, S.-J. Zhang, C. Pellicer, B. Wang, and E. Abdalla, *Physical Review D* **90**, 044042 (2014).
- [37] R. Konoplya and A. Zhidenko, *Physical Review D* **90**, 064048 (2014).
- [38] M. Abramowitz and I. A. Stegun, *Handbook of Mathematical Functions with Formulas, Graphs, and Mathematical Tables*, 9th ed. (Dover, New York City, 1964).
- [39] D.-P. Du, B. Wang, and R.-K. Su, *Physical Review D* **70**, 064024 (2004).
- [40] A. Y. Kazakov, *Journal of Physics A: Mathematical and General* **39**, 2339 (2006).
- [41] Y. Kwon, S. Nam, J.-D. Park, and S.-H. Yi, *Classical and Quantum Gravity* **28**, 145006 (2011).
- [42] B. Cuadros-Melgar, J. de Oliveira, and C. E. Pellicer, *Physical Review D* **85**, 024014 (2012).
- [43] S. Hod, *The European Physical Journal C* **C77**, 351 (2017).
- [44] R. Fontana, P. González, E. Papantonopoulos, and Y. Vásquez, *Physical Review D* **103**, 064005 (2021).
- [45] V. Cardoso, M. Lemos, and M. Marques, *Physical Review D* **80**, 127502 (2009).
- [46] S. Hod, *Physics Letters B* **786**, 217 (2018).
- [47] B. F. Schutz and C. M. Will, *Astrophysical Journal* **291**, L33 (1985).
- [48] S. Hod, *Physics Letters B* **796**, 256 (2019).
- [49] V. Ferrari and B. Mashhoon, *Physical Review D* **30**, 295 (1984).

- [50] E. Berti, V. Cardoso, and A. O. Starinets, *Classical and Quantum Gravity* **26**, 163001 (2009).
- [51] Y. Mo, Y. Tian, B. Wang, H. Zhang, and Z. Zhong, *Physical Review D* **98**, 124025 (2018).
- [52] R. A. Konoplya and A. Zhidenko, *Reviews of Modern Physics* **83**, 793–836 (2011).
- [53] K. Destounis, R. D. Fontana, and F. C. Mena, *Physical Review D* **102**, 044005 (2020).
- [54] V. Cardoso, J. L. Costa, K. Destounis, P. Hintz, and A. Jansen, *Physical Review Letters* **120**, 031103 (2018).